Int. J. Electrochem. Sci., 7 **(2012)** 8637 - 8647

International Journal of
ELECTROCHEMICAL
SCIENCE
www.electrochemsci.org

Electrochemical and Optoelectronic Characterization of Novel Poly[2,5-Dialkoxy-*p*-Phenyleneethynylene-2,7-(9,9-Fluorene)]s with 7-Oxy-4-Methylcoumarin Side Groups

Cheng-Jang Tsai[1,*], *Tzi-Yi Wu*[2], *Yun Chen*[3], *Chung-Wen Kuo*[4], *Shien-Jen Yang*[5]

[1] Department of Energy Application Engineering, Far East University, 74448 Tainan, Taiwan, ROC
[2] Department of Chemical and Materials Engineering, National Yunlin University of Science and Technology, Yunlin 64002, Taiwan, ROC
[3] Department of Chemical Engineering, National Cheng Kung University, 70101 Tainan, Taiwan
[4] Department of Chemical and Materials Engineering, National Kaohsiung University of Applied Sciences, Kaohsiung 80778, Taiwan, ROC
[5] Department of Cosmetic Applications & Management, Far East University, 74448 Tainan, Taiwan
[*]E-mail: jang@cc.feu.edu.tw

Received: 23 July 2012 / *Accepted:* 9 August 2012 / *Published:* 1 September 2012

Two new poly[2,5-dialkoxy-p-phenyleneethynylene-2,7-(9,9-dihexylfluorene)]s (PPEF) consisting of conjugated emitting chromophores of the backbone and pendant hexyloxy groups (**P1**) or pendant 7-oxygen-4-methylcoumarin (OMC) chromophores via flexible spacer (**P2**), have been successfully prepared and their electrochemical and optoelectronic properties are investigated. The emission of **P2** in solution is similar to model polymer (**P1**), and they show peak at 445 nm, which is attributed to PPEF backbone. Accordingly, efficient energy transfer from the OMC chromophores to PPEF backbone occurred readily in **P2**. The HOMO and LUMO energy levels of the two polymers have been estimated from their cyclic voltammograms. All the observations directly prove that the oxidation starts at the hole transporting segments of main chain. The electron affinity can be enhanced by introducing isolated electron-transporting side groups that lead to charges injection balance. The double layer polymer light-emitting diodes (PLED) of ITO/PEDOT:PSS /**P1**-**P2**/Ca:Al are fabricated, and they both emit yellow color light in electroluminescence (EL) spectra. Moreover, incorporation of OMC unit increases the electron affinity and reduces the turn-on electric field.

Keywords: Conjugated polymers, cyclic voltammograms, HOMO and LUMO energy level, electrochemically derived band gap, coumarin

1. INTRODUCTION

The electrochemical and optoelectronic properties of a number of different conjugated polymers have been investigated [1-17]. Among them, conjugated polymers contain phenylene [e.g.

poly(*p*-phenylene)s (PPP) [18], polyfluorene (PF)] [19], and phenylenevinylene [e.g. poly(*p*-phenylenevinylene) (PPV)] [20] in the conjugated backbone have been widely studied for electrochemical and optoelectronic applications, only a few groups studied the electrochemical and optoelectronic properties of phenyleneethynylene [e.g. poly(*p*-phenyleneethynylene)s (PPE) [21] and poly(2,7-9,9-di-2-ethylhexylfluorenylene ethynylene) (PFE) [22] in the conjugated polymers backbone, and they were generally not considered to be a promising emitting layer for OLED devices [23]. Moreover, the vast majority of conjugated polymers is insoluble and infusible in their pristine form, as a consequence of the rigid nature of the chains and the strong intermolecular interactions [24]. In order to enhance the solubility of rigid rod conjugated polymers, lateral substituents were attached to the backbone [25].

A literature survey revealed that a series of coumarin-terminated poly[2-methoxy-5-(2-ethylhexyloxy)-1,4-phenylenevinylene] (MEH-PPV) was synthesized by the Gilch methodology [26]. It has been shown that the end capping of this polymer with coumarin moieties is a convenient way of tuning the emission color and improving photoluminescent and electroluminescent efficiencies [26,27], poly(fluorenediyl vinylene)s with side chains containing coumarin moieties attached to the C-9 of fluorene through alkyl spacers also showed similar properties [28]. In substituted PPE with pendant OMC chromophores covalently attached to the conjugated polymer backbone, efficient resonance energy transfer was observed from the chromophores to the PPE backbone, resulting in enhanced luminescence of the PPE macromolecules [29].

In this work, two new polymers contained PPEF, PPE, and PFE conjugated backbone, and one covalently linked pendant chromophores (OMC) via a flexible spacer were synthesized and characterized. The fluorene unit was inserted to two novel polymers in order to improve the solubility of PPE conjugated backbone. OMC shows donating ability, whereas -C≡C-, coumarin, and fluorene units are electron deficient [30]. We attempted to balance the electron affinities and hole transporting ability in the polymer. The optical, EL, and electrochemical properties of two polymers have been investigated in detail.

2. EXPERIMENTAL

2.1. Materials and measurement

Monomers **1**, **2**, **3** and model compounds **M1** were synthesized and purified by procedures reported previously [29,31,32]. Tetrakis (triphenylphosphine) palladium [$Pd(PPh_3)_4$, Acros], copper (I) iodide (CuI, Aldrich), and iodobenzene (C_6H_5I, TCI) were purchased and used without further purification. Chloroform ($CHCl_3$, Tedia), diisopropylamine ($C_6H_{15}N$; Acros), and other solvents were HPLC grade reagents. The synthesized compounds were identified by ^1H NMR, FT-IR, and elemental analysis (EA). The ^1H NMR spectra were recorded on a Bruker AMX-400 MHz FT-NMR; and chemical shifts are reported in ppm using tetramethylsilane (TMS) as an internal standard. The FT-IR spectra were measured with a fourier transform infrared spectrometer, model Valor III from Jasco. The elemental analysis was carried out on a Heraus CHN-Rapid elemental analyzer. A Perkin Elmer TGA-

7 thermal analyzer was employed for the thermogravimetric analysis (TGA) of the polymers under nitrogen atmosphere at a heating rate of 20 °C/min. Thermal transitions of the polymers were measured using a differential scanning calorimeter (DSC), model DSC7 from Perkin Elmer, under nitrogen atmosphere at a heating rate of 10 °C/min. Absorption spectra were measured on a Jasco V-550 spectrophotometer and PL spectra were obtained using a Hitachi F-4500 spectrofluorometer. The cyclic voltammograms (CV) were measured with cyclic voltammeter, CV-50W from BAS, using a platinum disk electrode as the working electrode, an Ag/AgCl electrode as the reference electrode and a platinum wire electrode as the auxiliary electrode. The electrodes were supported in 0.1 M (n-$Bu)_4NClO_4$ in acetonitrile. The energy levels were calculated using the ferrocence (FOC) value of -4.8 eV with respect to vacuum level, which is defined as zero [33].

2.2. Fabrication and characterization of EL devices

Double-layer PLED devices (ITO/PEDOT:PSS/**P1**-**P2**/Ca/Al) were fabricated by successive spin-coating of hole-transporting poly(3,4-ethylenedioxythiophene) (PEDOT:PSS) and emitting polymers (**P1**, **P2**), and followed with vacuum deposition of metal cathode. The pretreatments of ITO glass included routine sonication in a detergent solution, distilled water, and isopropyl alcohol in sequence. The ITO glass (14 Ω/square) was first spin-coated (3000 rpm) with PEDOT:PSS solutions to obtain a film, heated in a vacuum oven at 150 °C for 15 min, and then it was coated (1000 rpm) with solutions of **P1** or **P2** (6-3 mg/ml in $CHCl_3$) to obtain a polymer layer. Finally, a thin layer of calcium (about 50 nm) covered with a thin layer of aluminum as the cathode was deposited in a vacuum thermal evaporator through a shadow mask at a pressure of less than 10^{-6} Torr. The active area of each device was about 4 mm^2. The device and EL spectra were operated and recorded with a combination of a Keithley model 2400 power supply and an Ocean Optics usb2000 spectrofluorometer in a glove box filled with N_2.

2.3. Polymer synthesis

A typical polymerization procedure described as follows: To a mixture of toluene (7 mL) and diisopropylamine (3 mL) were added with 2,7-diethynyl-9,9'-dihexylfluorene (**3**, 0.093 mg, 0.243 mmol), diiodo monomer (**1** or **2**: 0.223 mmol), iodobenzene (12 mg, 0.058 mmol), $Pd(PPh_3)_4$ (12.3 mg), and CuI (9 mg). The mixture was stirred at 75 °C for 2 h, added with iodobenzene (0.05 ml), and then stirred for another 22 h. The resulting strongly luminescent suspension was precipitated from methanol (200 ml) and the appearing purple precipitates were collected by filtration. The purple product was dissolved in $CHCl_3$ (3 mL), reprecipitated from methanol (300 mL), and dried in vacuo.

P1: FT-IR (KBr, pellet, cm^{-1}): ν 2928 (C-H), 2209 (C≡C), 2136 (C≡C), 1602, 1463, 1377, 1210 (C-O-C), 1014. ^1H NMR ($CDCl_3$, ppm): δ 7.67 (s, 2H, Ar H), 7.52 (s, 4H, Ar H), 7.24 (s, 2H, Ar H), 4.08-4.02 (d, 4H, $-CH_2-$), 1.97 (m, 8H, $-CH_2-$), 1.58-1.39 (m, 4H, $-CH_2-$), 1.05-0.78 (m, 26H, $-CH_2-$ and $-CH_3$), 0.6 (m, 10H, $-CH_2-$ and $-CH_3$). Elem. Anal. Calcd (%) for $C_{51}H_{68}O_2$: C, 85.90; H, 9.61. Found: C, 84.12; H, 8.3.

P2: FT-IR (KBr, pellet, cm^{-1}): ν 2927 (C-H), 2209 (C≡C), 2136 (C≡C), 1730 (lactone), 1613, 1461, 1387, 1207 (C-O-C), 1014. ^{1}H NMR ($CDCl_3$, ppm): δ 7.68 (d, 2H, Ar H), 7.52 (d, 4H, Ar H), 7.35 (d, 2H, Cou H-5), 7.19 (s, 2H, Ar H), 6.81-6.78 (m, 4H, Cou H-6, H-8), 6.13 (s, 2H, Cou H-3), 4.06-3.93 (t, 8H, $-CH_2-$), 2.39 (s, 6H, Cou-CH_3), 1.95 (m, 4H, $-CH_2-$), 1.87(m, 8H, $-CH_2-$), 1.58 (m, 8H, $-CH_2-$), 1.05 (m, 12H, $-CH_2-$), 0.68 (t, 6H, $-CH_3$), 0.58 (m, 4H, $-CH_2-$). Elem. Anal. Calcd (%) for $C_{67}H_{72}O_8$: C, 80.05; H, 7.22. Found: C, 78.84; H, 7.84.

3. RESULTS AND DISCUSSION

3.1. Synthesis and thermal properties

The new conjugated copolymers **P1** and **P2** were prepared from diiodo monomers (**1**, **2**) and 2,7-diethynyl-9,9'-dihexylfluorene (**3**) by the Heck cross-coupling reaction (Scheme 1) using $Pd(PPh_3)_4$ and CuI as the catalysts. To control the molecular weight of the polymers, the ratio of the bifunctional monomers was carefully adjusted. In addition, iodobenzene was added as end-capping reagent to ensure that the polymers have well-defined, non-reactive end groups [29]. The yields and characterized data of the **P1** and **P2** are summarized in Table 1. The weight-average molecular weights (M_w) of **P1** and **P2**, determined by gel permeation chromatography using mono-dispers polystyrene as standard, were 9150 and 20470, respectively, with polydispersity indexes being in the range of 2.09 - 3.80 (Table 1). The copolymers are soluble in common organic solvents such as chloroform, dichoromethane, toluene, and *N*,*N*-dimethylformamide (DMF). The solubility of **P1** and **P2** are much better than PPE, which can be attributed to the alkyl side groups attached to both phenylene and fluorene units. The thermal decomposition temperatures (T_d: at 5% weight loss) were 354 °C and 290 °C for **P1** and **P2**, respectively, indicating that the former without OMC group show better thermal stability than **P2**. Neither melting temperature nor glass transition temperature was observed below 250 ºC on their differential scanning calorimetric (DSC) thermograms, these results suggest the **P1** and **P2** are basically amorphous copolymers with modest thermal stability.

Table 1. Preparation and properties of **P1** and **P2**.

No.	Yield (%)	M_w [a]	PDI [a]	T_d [b] (°C)
P1	53.3	9150	2.09	354
P2	48.3	20470	3.80	290

[a] M_w and PDI of the polymers were determined by gel permeation chromatography using mono-disperse polystyrene as standards; eluent: $CHCl_3$.

[b] Decomposition temperature at 5 % weight loss was measured by TGA at a heating rate of 20 °C/min under nitrogen.

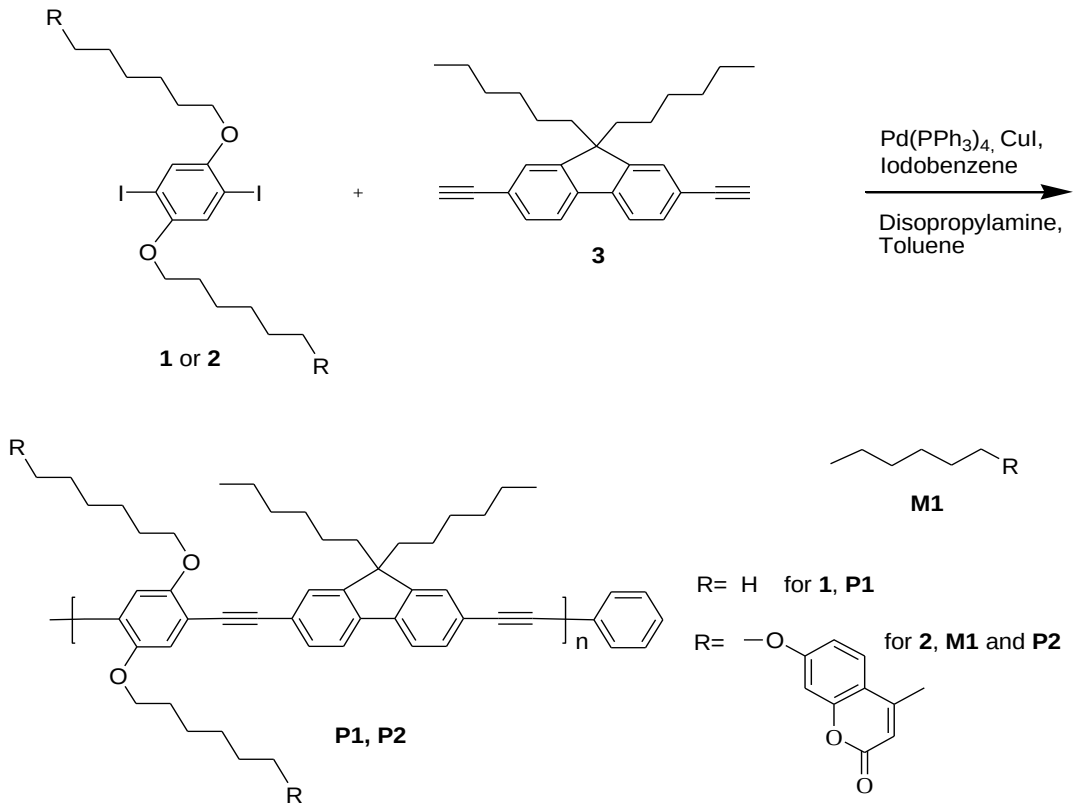

Scheme 1.

3.2. Optical properties

We study the optical properties of 4-methylcoumarin derivative (**M1**), **P1**, and **P2**. **P1** is the model polymer corresponding to emitting conjugated backbone of **P2**, whereas **M1** corresponds to the OMC chromophores of side chain [34]. Figure 1 exhibits the absorption and PL spectra of **M1**, **P1**, and **P2** in chloroform, and the corresponding absorption and emission maxima are listed in Table 2. The absorption spectra maxima of **P2** situate around 330 nm and 400 nm, which are basically the overlap of those of **M1** and **P1**, whereas the PL spectra of **P1** and **P2** (under excitation at 320 nm) show similar shape with one main PL peak at 446 nm. Although **P2** contains extra electron-transport pendant OMC groups, the PL band of electron-transporting chromophores at ca. 380 nm disappears completely. Therefore, the PL spectrum of **P2** is mainly dominated by the fluorophores with longer emissive wavelength (emitting backbone), indicating that efficient excitation energy transfer from electron-transporting OMC to conjugated backbone has occurred in **P2** under photo-excitation. The emission spectrum of **M1** is similar to the absorption spectra of **P1** (Figure 1), this suggests that excitation energy might transfer from **M1** (energy donor) to **P1** (energy acceptor) if the distance between the donor and acceptor is close sufficiently. As shown in Figure 2, the PL spectrum of the mixture of **M1** and **P1** (excited at 320 nm) exhibits emission peaks at 380 nm and 446 nm, the relative emission intensity of **P1** (at ca. 446 nm) to that of **M1** (at ca. 380 nm) enhances significantly with increasing concentration (from 1×10^{-5} M to 1×10^{-4} M). The transformation of PL spectra with concentration

would be caused by increasing re-absorption and excitation energy transfer due to reduced intermolecular distance that is mainly controlled by the concentration in solution.

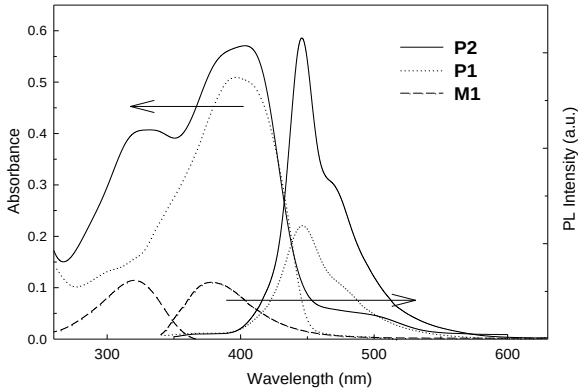

Figure 1. Absorption and photoluminescence spectra (excitation at 320 nm) of **P1**, **P2**, and **M1** in $CHCl_3$ (1×10^{-5} M).

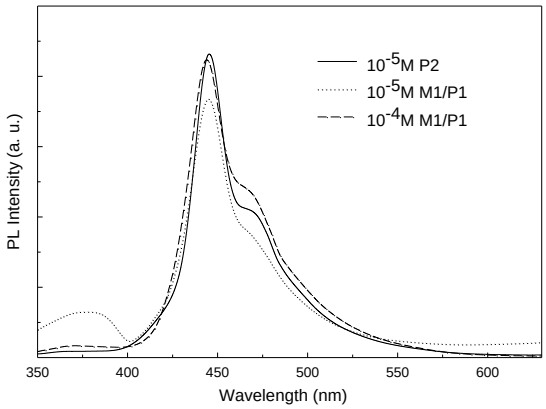

Figure 2. Photoluminescence spectra (excitation at 320 nm) of **P2** (1×10^{-5} M) and mixture of **M1** and **P1** (1×10^{-4} M, 1×10^{-5} M) in $CHCl_3$.

Table 2. Optical Properties of **P1** and **P2.**

No.	UV-vis λ_{max} (nm)[a]		PL λ_{max} (nm)[a]		Φ_{PL}[b]
	soln.	Film	soln.	film	soln.
P1	400	414	446	450, 550	0.57
P2	330, 400	330, 412	446	450, 550	0.60

[a] The solvent for solution preparation and spin-coating is chloroform for **P1** and **P2**.

[b] These values were measured by using quinine sulfate (dissolved in 1 N $H_2SO_{4(aq)}$ with a concentration of 10^{-6} M, assuming Φ_{PL} of 0.55) as a standard. The excitation wavelength were 320 nm for **P1** and **P2** solutions (10^{-6} M repeating unit), which had a absorbance less than 0.05.

The PL spectra of **P2** show mainly the emission of hole-transporting PPEF main chain at 446 nm (Figure 2), this can be attributed to efficient intramolecular energy transfer because the energy donor (coumarin side chain) and the energy acceptor (PPEF backbone) are connected via a flexible spacer. The relative quantum yields (Φ_{PL}) of **P1** and **P2** in chloroform are 0.57 and 0.60, respectively. Energy transfer between donor and acceptor (sensitizer and emitting segments) also affects the relative quantum yields of **P2** [35].

The PL spectra of both **P1** and **P2** films show a broad and intense peak (550 nm) in the yellow region (Figure 5), which is usually attributed to aggregate/excimer emission or fluorenone defect [36]. In addition, a small luminescence peak (450 nm) in the blue region is still observed for **P1** and **P2**, which is residue emission of PPEF.

3.3. Electrochemical property

Cyclic voltammetry (CV) was employed to investigate the redox potentials, and then to estimate the HOMO and LUMO energy levels of **P1** and **P2** [37-44]. The cyclic voltammograms (CV) of **P1** and **P2** are shown in Figure 3 and their electrochemical data are summarized in Table 3. The onset oxidation potentials (versus FOC) of **P1** and **P2** are almost the same (0.80 and 0.79 V) because they contain the same hole-transporting PPEF backbone. However, their onset reduction potentials are very different and located at -2.05V and -1.38V, respectively. The **P2** is reduced much more easily than **P1** due to the isolated electron-transporting OMC side groups. The estimated HOMO and LUMO energy levels of **P2** are -5.59 eV and -3.42 eV, whereas those of **P1** are -5.60 eV and -2.75 eV, respectively. Obviously, the OMC groups enhance electron affinity of **P2** significantly by reducing its LUMO level from -2.55 eV of **P1** to -3.42 eV. Moreover, a large energy gap (2.85 eV) of **P1** indicates that the incorporation of ethynylene in the main chain shortens the effective conjugation length [45].

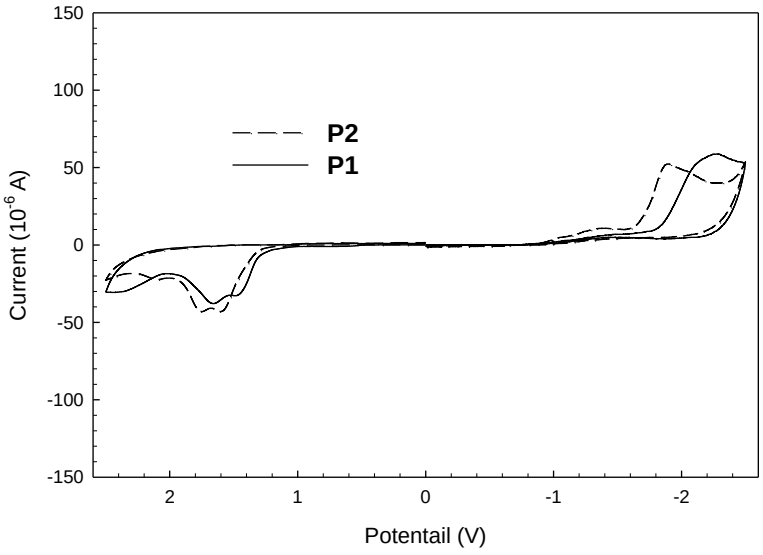

Figure 3. Cyclic voltammograms of **P1** and **P2** films coated on platinum working electrode. Scanning rate: 50 mV/s.

The optical band gap (E_g^{opt}) of **M1** and model polymer (**P1**), calculated from their edge absorption, are 3.25 and 2.75 eV, respectively [31,46]. Therefore, the unabridged energy band of **P2** can be proposed as shown in Figure 4. The LUMO levels of hole-transporting backbone can be estimated from the HOMO levels of **P2** by adding the E_g^{opt} of the corresponding model polymer (**P1**). According, the LUMO level of hole-transporting PPEF backbone in **P2** is estimated to be -2.84 eV by the E_g^{opt} of the corresponding **P1** (2.75 eV) and its HOMO level (-5.59 eV). The electrochemically-determined energy band of **P2** is the overlapped portions of corresponding models **M1** and **P1**. Therefore, electron affinity of **P2** can be promoted significantly by electron-withdrawing OMC groups. In general, the decrease in LUMO levels enhances electron affinity and leads to reduced electron-injection barriers. Therefore, the electron- and hole-injection would be balanced in **P2** when employed **P2** as the emitting layer in EL devices.

Table 3. Electrochemical Data of **P1** and **P2**.

No.	$E_{onset(ox)}$ vs. Ag/AgCl(V)	$E_{onset(red)}$ vs. Ag/AgCl(V)	$E_{onset(ox)}$ vs. E_{FOC}(V)[a]	$E_{onset(red)}$ vs. E_{FOC}(V)[a]	E_{HOMO} (eV)[b]	E_{LUMO} (eV)[c]	E_g^{el} (eV)[d]
P1	1.25	-1.60	0.80	-2.05	-5.60	-2.75	2.85
P2	1.26	-0.93	0.79	-1.38	-5.59	-3.42	2.20

[a] ($E_{onset(ox\ or\ red)}$ vs. E_{FOC}) = ($E_{onset(ox\ or\ red)}$ vs. Ag/AgCl(V))- E_{FOC}, E_{FOC} = 0.45 V vs. Ag/AgCl.

[b] E_{HOMO}= -e($E_{onset(ox),\ FOC}$ + 4.8 V).

[c] E_{LUMO}= -e($E_{onset(red),\ FOC}$ + 4.8 V).

[d] Band gaps obtained from electrochemical data: E_g^{el} = E_{LUMO} - E_{HOMO}.

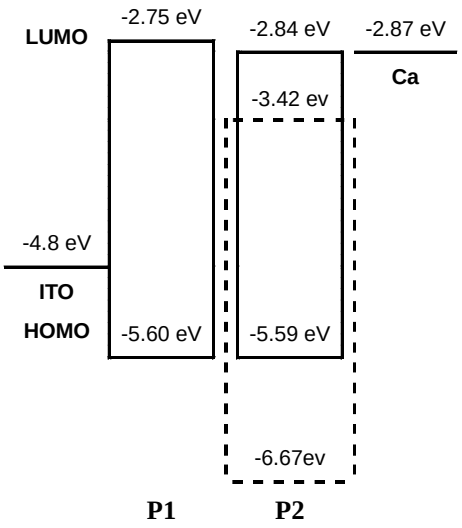

Figure 4. Energy band diagram of **P1** and **P2** (emitting segments: — ; electron- transporting segments: - - -).

3.4. Double-layer LED device

Double-layer light emitting diodes (ITO/PEDOT:PSS/**P1**-**P2**/Ca:Al) were fabricated for optoelectronic investigation. The EL spectrum of **P2** shows only the emission of PPEF backbone and no emission of the side OMC moieties can be observed at blue–violet region even at high voltages (Figure 5). The EL maxima of **P1** and **P2** devices locate at 547 nm and 544 nm, respectively, the features are similar to those observed in PL spectra of the corresponding polymer films. Double-layer EL devices of both **P1** (CIEx,y= 0.32, 0.48) and **P2**(CIEx,y= 0.34, 0.46) emit yellow light. Figure 6 shows the current density (J)-voltages (V)-luminance (L) diagram of the devices. The turn-on voltages for current density are 5 and 3 V with luminance maxima of 34 and 58 cd/m^2 for **P1** and **P2**, respectively. The **P2** film shows lower turn-on voltages (for current density) and greater luminance maxima, which can be attributed to enhanced electron injection due to electron-withdrawing OMC groups and occurrence of energy transfer from OMC to emitting PPEF backbone.

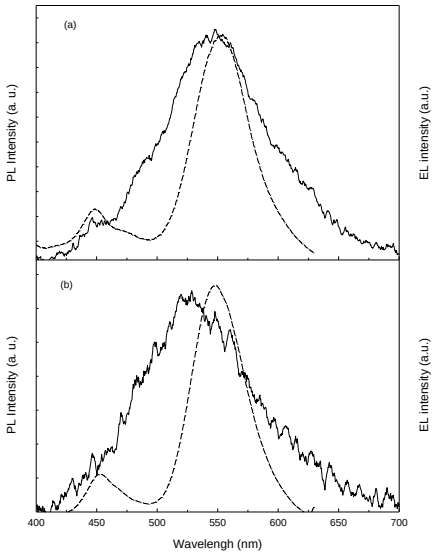

Figure 5. Electroluminescenct spectra (solid line) and photoluminescent spectra (excitation at 320 nm) (broken line) of (a) **P1** and (b) **P2** in film state.

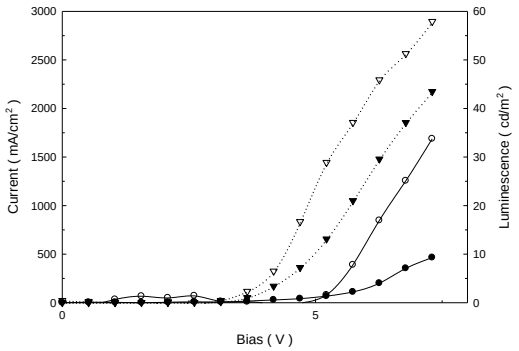

Figure 6. The luminance vs. bias (hollow) and current density vs. bias (full) characteristics for the devices of the double layer devices of ITO/PEDOT:PSS/**P1**/Ca:Al (circle) and ITO/PEDOT:PSS/**P2**/Ca:Al (triangle).

4. CONCLUSIONS

We have successfully prepared two PPEF derivatives **P1** (as model polymer) and **P2** by typical Heck reaction. The solubility of **P1** and **P2** are much better than PPE, which can be attributed to the alkyl side groups attached to both phenylene and fluorene units. Corresponding model compound **M1** of pendant OMC group have also prepared for comparison. The emission in **P2** is mainly attributed to PPEF main chain due to efficient energy transfer from electron-transporting OMC chromophores. From the analysis of electrochemical experiment, electron affinity of **P2** is enhanced by OMC chromophores. Double-layer EL devices of both polymers emit yellow light, and **P2** device showed lower turn-on electric fields and greater maxima luminance, which can be attributed to enhanced electron injection due to electron-withdrawing OMC groups.

ACKNOWLEDGEMENTS
The authors would like to thank the National Science Council of the Republic of China for financially supporting this project.

References

1. R.H. Friend, R.W. Gymer, A.B. Holmes, J.H. Burroughes, R.N. Marks, C. Taliani, D.D.C. Bradley, D.A. Dos Santos, J.L. Brédas, M. Lögdlund, W.R. Salaneck, *Nature*, 397 (1999) 121.
2. Y. Chen, T.Y. Wu, *Polymer*, 42 (2001) 9895.
3. X.H. Zhu, L.Y. Xu, M. Wang, Z. Wang, R.M. Liu, J.S. Zhao, *Int. J. Electrochem. Sci.*, 6 (2011) 1730.
4. T.Y. Wu, Y. Chen, *J. Polym. Sci. A Polym. Chem.*, 40 (2002) 3847.
5. Q.X. Wang, X.L. Wang, Z.L. Yu, X.L. Yuan, K. Jiao, *Int. J. Electrochem. Sci.*, 6 (2011) 5470.
6. T.Y. Wu, Y. Chen, *J. Polym. Sci. A Polym. Chem.*, 40 (2002) 4570.
7. A.C. de Sa, L.L. Paim, U.D. Bicalho, D.R. do Carmo, *Int. J. Electrochem. Sci.*, 6 (2011) 3754.
8. T.Y. Wu, Y. Chen, *J. Polym. Sci. A Polym. Chem.*, 40 (2002) 4452.
9. R.A. Olowu, A. Williams, P.M. Ndangili, R.F. Ngece, S.N. Mailu, P. Baker, E. Iwuoha, *Int. J. Electrochem. Sci.*, 6 (2011) 1855.
10. T.Y. Wu, Y. Chen, *J. Polym. Sci. A Polym. Chem.*, 41 (2003) 1444.
11. D.P. dos Santos, M.F. Bergamini, M.V.B. Zanoni, *Int. J. Electrochem. Sci.*, 5 (2010) 1399.
12. T.Y. Wu, N.C. Lee, Y. Chen, *Synth. Met.*, 139 (2003) 263.
13. C.W. Kuo, Z.Y. Kuo, J.J. Jow, T.Y. Wu, J.Y. Chen, X.X. Zhu, *Int. J. Electrochem. Sci.*, 7 (2012) 4974.
14. T.Y. Wu, Y. Chen, *J. Polym. Sci. A Polym. Chem.*, 42 (2004) 1272.
15. C.C. Yang, T.Y. Wu, H.R. Chen, T.H. Hsieh, K.S. Ho, C.W. Kuo, *Int. J. Electrochem. Sci.*, 6 (2011) 1642.
16. T.Y. Wu, R.B. Sheu, Y. Chen, *Macromolecules*, 37 (2004) 725.
17. C.W. Kuo, C.C. Yang, T.Y. Wu, *Int. J. Electrochem. Sci.*, 6 (2011) 3196.
18. P. Kovacic, M.B. Jones, *Chem. Rev.*, 87 (1989) 357.
19. G. Klaerner, R.D. Miller, *Macromolecules*, 31 (1998) 2007.
20. J.H. Burroughes, D.D.C. Bradley, A.R. Brown, R.N. Marks, K. Mackay, R.H. Friend, P.L. Burns, A.B. Holmes, *Nature*, 347 (1990) 539.
21. A. Montali, P. Smith, C. Weder, *Synth. Met.*, 97 (1998) 123.
22. X. Zhan, Y. Liu, D. Zhu, W. Huang, Q. Gong, *Chem. Mater.*, 13 (2001) 1540.

23. A. Kraft, A.C. Grimsdale, A.B. Holmes, *Angew. Chem. Int. Ed.*, 37 (1998) 403.
24. P. Wautelet, M. Moroni, L. Oswald, J.L. Moigne, A. Pham, J.Y. Bigot, *Macromolecules*, 29 (1996) 446.
25. Y. Watanabe, T. Mihara, N. Koide, *Macromol. Chem. Phys.*, 199 (1998) 977.
26. Y. Huang, Z.Y. Lu, Q. Peng, Q. Jiang, R.G. Xie, S.H. Han, L.G. Dong, J.B. Peng, Y. Cao, M.G. Xie, *Macromol. Chem. Phys.*, 93 (2005) 95.
27. Y. Huang, Z.Y. Lu, Q. Peng, R.G. Xie, M.G. Xie, J.B. Peng, Y. Cao, *J. Mater. Sci.*, 40 (2005) 601.
28. V.P. Barberis, J.A. Mikroyannidis, V. Cimrová, *J. Polym. Sci. A Polym. Chem.*, 44 (2006) 5752.
29. A.R.A. Palmans, P. Smith, C. Weder, *Macromolecules*, 32 (1999) 4677.
30. W. Huang, S. Wang, H. Yang, Q. Gong, X. Zhan, Y. Liu, D. Zhu, *Chem. Phys. Lett.*, 350 (2001) 99.
31. Y. Chen, S.W. Hwang, Y.H. Yu, *Polymer*, 44 (2003) 3827.
32. S.H. Lee, T. Nakamura, T. Tsutsui, *Org. Lett.*, 3 (2001) 2005.
33. Y. Liu, M.S. Liu, A.K.Y. Jen, *Acta. Polym.*, 50 (1999) 105.
34. S.W. Hwang, Y. Chen, *Macromolecules*, 35 (2002) 5438.
35. C.J. Tsai, K.M. Yeh, Y. Chen, *J. Polym. Sci. A Polym. Chem.*, 45 (2007) 211.
36. X. Chen, H.E. Tseng, J.L. Liao, S.A. Chen, *J. Phys. Chem. B*, 109 (2005) 17496.
37. H. Mohammad-Shiri, M. Ghaemi, S. Riahi, A. Akbari-Sehat, *Int. J. Electrochem. Sci.*, 6 (2011) 317.
38. T.Y. Wu, M.H. Tsao, F.L. Chen, S.G. Su, C.W. Chang, H.P. Wang, Y.C. Lin, W.C. Ou-Yang, I.W. Sun, *Int. J. Mol. Sci.*, 11 (2010) 329.
39. S. Riahi, M.R. Ganjali, H. Khajehsharifi, P. Norouzi, S. Taghipoor, *Int. J. Electrochem. Sci.*, 4 (2009) 122.
40. T.Y. Wu, M.H. Tsao, F.L. Chen, S.G. Su, C.W. Chang, H.P. Wang, Y.C. Lin, I.W. Sun, *J. Iran. Chem. Soc.*, 7 (2010) 707.
41. D. Nematollahi, A. Taherpour, S. Jameh-Bozorghi, A. Mansouri, B. Dadpou, *Int. J. Electrochem. Sci*. 5 (2010) 867.
42. M.H. Tsao, T.Y. Wu, H.P. Wang, I.W. Sun, S.G. Su, Y.C. Lin, C.W. Chang, *Mater. Lett.*, 65 (2011) 583.
43. S. Jameh-Bozorghi, M. Darvishpour, S. Mostghiman, Z. Javanshir, *Int. J. Electrochem. Sci.*, 6 (2011) 4891.
44. T.Y. Wu, M.H. Tsao, S.G. Su, H.P. Wang, Y.C. Lin, F.L. Chen, C.W. Chang, I.W. Sun, *J. Braz. Chem. Soc.*, 22 (2011) 780.
45. L. Akcelrud, *Prog. Polym. Sci.*, 28 (2003) 875.
46. S.W. Hwang, S.H. Chen, Y. Chen, *J. Polym. Sci. A Polym. Chem.*, 40 (2002) 2215.